Published in final edited form as:
Circ Res. 2010 May 28; 106(10): 1570–1581. doi:10.1161/CIRCRESAHA.109.212589.

Magnetic Targeting Enhances Engraftment and Functional Benefit of Iron-Labeled Cardiosphere-Derived Cells in Myocardial Infarction

Ke Cheng, PhD, **Tao-Sheng Li, MD, PhD**, **Konstantinos Malliaras, MD**, **Darryl Davis, MD**, **Yiqiang Zhang, PhD**, and **Eduardo Marbán, MD, PhD**

Abstract

Rationale—The success of cardiac stem cell therapies is limited by low cell retention, due at least in part to washout via coronary veins.

Objective—We sought to counter the efflux of transplanted cells by rendering them magnetically-responsive and imposing an external magnetic field on the heart during and immediately after injection.

Methods and Results—Cardiosphere-derived cells (CDCs) were labeled with superparamagnetic microspheres (SPMs). *In vitro* studies revealed that cell viability and function were minimally affected by SPM labeling. SPM-labeled rat CDCs were injected intramyocardially, with and without a superimposed magnet. With magnetic targeting, cells were visibly attracted towards the magnet and accumulated around the ischemic zone. In contrast, the majority of non-targeted cells washed out immediately after injection. Fluorescence imaging revealed more retention of transplanted cells in the heart, and less migration into other organs, in the magnetically-targeted group. Quantitative PCR confirmed that magnetic targeting enhanced cell retention (at 24 hours) and engraftment (at 3 weeks) in the recipient hearts by ~3-fold compared to non-targeted cells. Morphometric analysis revealed maximal attenuation of LV remodeling, and echocardiography showed the greatest functional improvement, in the magnetic targeting group. Histologically, more engrafted cells were evident with magnetic targeting, but there was no incremental inflammation.

Conclusion—Magnetic targeting enhances cell retention, engraftment and functional benefit. This novel method to improve cell therapy outcomes offers the potential for rapid translation into clinical applications.

Keywords

cardiac progenitor cells; cell transplantation; myocardial infarction; targeted cell delivery

Corresponding Author: Eduardo Marbán, MD, PhD, Address: The Heart Institute, Cedars-Sinai Medical Center, 8700 Beverly Blvd, 1090 Davis Building, Los Angeles, CA 90048, Fax: 310 423 7637, Tel: 310 423 7998, Eduardo.Marban@csmc.edu.

Disclosures: Dr. Marbán is a founder and equity holder in Capricor Inc. Capricor provided no funding for the present study. The remaining authors report no conflicts.

Introduction

Stem cell transplantation is a promising therapeutic strategy for acute or chronic ischemic cardiomyopathy [1]. Low cell retention and engraftment are major obstacles to achieving a significant functional benefit irrespective of the cell type or model used [2, 3]. Acute (≤24 hour) cell retention is normally less than 10%, regardless of the delivery route [3]. Initial studies highlighted apoptosis as the culprit underlying low engraftment[4, 5], but recent work has shown that venous drainage and the contraction of a beating heart account for significant loss of transplanted cells[6, 7]. As short-term cell retention is a prerequisite for long-term cell engraftment and functional improvement, translatable methods to attenuate cell loss are highly desirable. Magnetic targeting represents a non-invasive approach to coax therapeutic agents (e.g. drugs, cells) into desired regions[8]. In the cardiovascular arena, previous work has concentrated on endothelial cell-related therapies, using magnetic targeting to improve cell homing to grafts or stents[9-15]. Moreover, previous studies have evaluated only short-term cell retention, not long-term engraftment or functional benefits[9-15].

Here, we examine myocardial rather than endothelial targeting, and quantify long-term cardiac engraftment and function after intramyocardial injection of iron-labeled cardiosphere-derived cells (CDCs) subjected to an external magnetic attractor.

Methods

An expanded Materials and Methods section can be found in the online data supplement at http://circres.ahajournals.org.

CDC Culture and SPM Labeling

CDCs were cultured from tissue samples of hearts explanted from 8-week-old male Wistar Kyoto (WKY) rats, as previously described[16-18]. CDCs were labeled with fluorescent (dragon green or flash red) superparamagnetic microsphere (SPM) particles (0.9 μm diameter; Bangs Laboratories) by co-incubation in culture for 24 hours. Loading of SPMs into CDCs was confirmed by Prussian Blue staining[19] and dragon green fluorescence. Labeling efficiency was assessed by flow cytometry.

Effects of SPM Labeling on CDC Properties

In vitro toxicity experiments were performed 24 hours after SPM labeling. Cell viability was assessed by Trypan Blue exclusion. Apoptosis and necrosis were assessed by flow cytometry (7AAD and Annexin-V stain)[16]. Methods used to assess cell proliferation and attachment are described in Detailed Methods. Percentages of cells that expressed the antigens c-kit, CD31, CD34 and CD90 were assessed by flow cytometry[16]. The apoptotic/necrotic effects of SPM labeling were examined by TUNEL staining[20]. H_2O_2-treated cells and non-treated cells were routinely included as positive and negative controls, respectively. Reactive oxygen species (ROS) generation was measured by two commercially available kits following manufacturers' protocols.

In vitro Cell Capture Experiments

SPM-labeled CDCs (500:1 SPM:cell ratio) were re-suspended in PBS (1 million cells/mL) in a 15 mL conical tube. A 1.3 Tesla magnet was applied directly to the outside tube wall or 1 cm away from the tube for 20 seconds. Cell condensation was assessed visually. To better simulate the contracting and turbulent environment of myocardium, the same magnet was mounted on the outside wall of a cell suspension tube which was rotated at 60 RPM. After 24 hours, cell condensation by magnetic capturing was visually examined.

Cell Injection and Magnetic Targeting

Animal care was in accordance to Institutional Animal Care and Use Committee guidelines. Female WKY (n=88 total) rats underwent left thoracotomy under general anesthesia, and myocardial infarction (MI) was produced by permanent ligation of the left anterior descending coronary artery. The animals were subjected to intramyocardial injections with a 29-gauge needle at four points in the infarct border zone, with one of the following randomly-assigned conditions: 1) Fe-CDC+Magnet group: injection of 1 million SPM-labeled cells in 100 μL PBS with a 1.3 Tesla magnet applied above the apex during the injection and for 10 min after injection; 2) Fe-CDC group: injection of 1 million SPM-labeled cells in 100 μL PBS without magnet application; 3) CDC group: injection of 1 million non-labeled cells in 100 μL PBS with magnet applied above the apex during the injection and for another 10 min after injection; and 4) Control group: injection of 100 μL PBS without cells. A SPM control group was subsequently added: injection of 5×10^8 SPM beads (no cells) in 100 μL PBS with magnet applied. A camcorder was attached to the surgical microscope to capture videos during cell injection.

Quantification of Engraftment by Real Time PCR

Male CDCs were injected into female rats, enabling detection of the SRY gene (located on the Y chromosome) as an index of engraftment. Quantitative real-time PCR was performed 24 hours and 3 weeks after cell injection (n=6 for each cell-injected group).

Fluorescence Imaging (FLI)

CDCs were labeled with SPMs that were conjugated with flash-red fluorophores (excitation: 660 nm; emission: 690 nm). Due to its long wavelength, flash-red is superior to dragon-green for imaging purposes. Hearts, lungs and spleens from representative animals from each group were harvested and imaged with the IVIS 200 (Xenogen) system to detect flash-red fluorescence. Hearts were washed with PBS to remove any cells adherent to the epicardium prior to imaging. Fluorescence signals (photon/s) from a fixed region of interest (ROI) were measured as described[21].

Echocardiography

To assess global cardiac function in 53 rats (Fe-CDC+Magnet [n =12], Fe-CDC [n =12], CDC [n=11], PBS control [n=9] and SPM control [n=9]), echocardiography was performed with the Vevo 770 system (Visual Sonics, Toronto, Canada) on day 0 post-MI and 3 weeks post-MI. The left ventricular ejection fraction (LVEF) was measured from the parasternal long-axis view. LVEF was calculated with Visual Sonics V1.3.8 software from 2D long-axis views taken through the infarcted area. Both absolute values and changes from baseline (day 0 post-MI) are reported.

Morphometric and Histology Analysis

Subpopulations of CDCs from each group were virally-transduced to express green fluorescent protein (GFP)[18]. In these cases, flash-red-conjugated SPMs were used to avoid crossover with the fluorescence of GFP. Animals receiving GFP cells and flash-red SPMs were sacrificed 3 weeks after injection. Hearts were cryo-sectioned and representative slides from each depth range were selected for immuohistochemistry. Quantitative morphometry analysis was performed as previously described[22].

Statistical Analysis

Results are presented as mean ± SD unless specified otherwise. Statistical significance between baseline and 3 week LVEFs was determined using 2-tailed paired Student's *t* test. All the other

comparisons between any 2 groups were performed using 2-tailed unpaired Student's *t* test. Comparison among more than 2 groups was analyzed by One-Way ANOVA followed by Bonferroni post hoc test. Differences were considered statistically significant when $p<0.05$.

Results

SPM Labeling Minimally Affects Cell Viability and Function

CDCs were labeled with Dragon-green fluorescence-conjugated SPM particles by co-incubation in culture for 24 hours. Prussian Blue staining and fluorescence microscopy confirmed particle uptake by CDCs (Figs. 1A and B). Non-labeled cells did not exhibit Prussian Blue or Dragon-green fluorescence (Insets, Figs. 1A and B). These labeled cells are hereafter called SPM-labeled CDCs, or Fe-CDCs for short. Flow cytometry revealed an average labeling efficiency of 86.4±1.2% when a 500:1 SPM:cell ratio was used. The number of $TUNEL^{POS}$ apoptotic cells increased with escalating SPM:cell ratio (red cells with white arrowheads Figs. 2A-C; Online Fig. I). From the same images, it is also obvious that more SPMs (green color) were taken up by each cell at higher SPM dosages. Figs. 2D and E show typical Annexin/7-AAD flow cytometry plots. Further quantification (Fig. 2F) indicated that SPM labeling induced <1% increase of apoptotic cells, but the SPM-labeled group had fewer necrotic cells. Given the fact that 500:1 labeling caused minimal cytotoxicity, this dosage was chosen for subsequent *in vitro* and *in vivo* experiments. Figs. 2G-J show that labeling with SPMs did not affect cell viability, proliferation, adhesion or antigenic phenotype of CDCs. In addition, SPM labeling did not lead to the generation of intracellular reactive oxygen species (ROS) (Online Fig. II).

External Magnet Captures SPM-Labeled CDCs *In Vitro*

To investigate the ability of a magnet to capture SPM-labeled CDCs *in vitro*, CDCs were loaded with 500:1 SPMs and re-suspended in a conical tube (Online Fig. IIIA). After applying the magnet directly on the outer wall of the tube, CDCs were rapidly attracted towards the magnet and accumulated focally on the adjacent inner wall (Online Fig. IIIB). To gauge the effect of a more remote magnetic field, the magnet was moved 1 cm away from the tube and the capture experiment was repeated. SPM-labeled CDCs were still rapidly attracted towards the magnet and attached focally, albeit with smaller cell condensates (Online Fig. IIIC). To better mimic the myocardial environment, where turbulent flow exists, the same magnet was mounted on the outside of a rotating tube containing Fe-CDC suspension. Without the magnet, the cell suspension was uniform, with no focal condensation (Online Fig. IIID). However, with the external magnet, Fe-CDCs formed a distinct condensate on the inner wall adjacent to the magnet (Online Fig. IIIE).

Magnetic Targeting Captures Fe-CDCs During Injection and Attenuates Washout Effect

One million CDCs derived from syngeneic male WKY rats were injected intramyocardially into the peri-infarct region of female hearts. White light imaging revealed that the majority of SPM-labeled CDCs (evident from their yellow-brown color) washed out within seconds (Online Movie I), diffusing from the injection site towards the base and then quickly disappearing. This confirms our prior conclusion[6] that initial washout accounts for significant cell loss. In contrast, Fe-CDCs injected with a magnet placed ~1 cm above the cardiac apex moved towards the apex and accumulated around the infarct (Online Movie II). As seen in the movies, more cells are visible after injection in a heart from the Fe-CDC + Magnet group (A) than in the Fe-CDC group (B). Thus, the external magnetic force was capable of effectively opposing the hydraulic forces that ordinarily drive washout.

Magnetic Targeting Improves Short-Term Retention and Long-Term Engraftment

Six animals from each cell-injected group were sacrificed 24 hours after cell injection to assess short-term cell retention. Visual inspection of the excised hearts revealed that the Fe-CDC + Magnet group (Fig. 3B; red arrow) had more cells around the injection area than did the Fe-CDC group (Fig. 3A). Likewise, representative FLI images revealed more flash-red fluorescence in a heart from the Fe-CDC + Magnet group (Fig. 3F) than in the Fe-CDC group (Fig. 3C). To compare off-target migration, lungs and spleens from the same animals were also harvested and imaged. Not surprisingly, red fluorescence signals were detectable in the lungs, but less so in the lungs from the Fe-CDC + Magnet group (Fig. 3G) than in those from the Fe-CDC group (Fig. 3D). Thus, the magnet retains CDCs in the heart, CDCs which otherwise end up elsewhere due to venous dispersion. The fluorescence seen in the Fe-CDC spleen (Fig. 3E) may reflect off-target CDCs, or clearance of SPM particles by spleen macrophages. In either case, such fluorescence is markedly reduced in the Fe-CDC + Magnet spleen (Fig. 3H). As a negative control, excised organs from the CDC group (animals injected with non-labeled cells) were also imaged. No signals were detectable in any organs (Figs. 3I-K).

To further assess the numbers of surviving CDCs in the myocardium, quantitative PCR for the male-specific SRY gene was performed. qPCR results confirmed that magnetic targeting enhanced short-term cell retention in the recipient hearts: the Fe-CDC + Magnet group exhibited ~3-fold greater cell numbers than the Fe-CDC group (Fig. 4A). Cell retention was indistinguishable in the Fe-CDC group and the CDC group, confirming the lack of an effect of labeling per se. To examine the effect of magnetic targeting on long-term engraftment, subsets of animals in each group were followed for 3 weeks and then sacrificed for qPCR and FLI. Consistent with previous findings[19, 23], PCR results indicated that all three groups experienced a huge decrease from the 24 hour time point. However, the Fe-CDC + Magnet group still exhibited enhanced cell engraftment relative to the Fe-CDC group (Fig. 4B). Again, SPM labeling itself did not affect engraftment, as the Fe-CDC group was comparable to the CDC group. The equivalence of the CDC and Fe-CDC groups at 24 hours (Fig. 4A) and 3 weeks (Fig. 4B) confirms the idea that SPM labeling does not affect cell proliferation *in vivo*, assuming the attrition rate of transplanted CDCs is identical in the two groups. FLI images showed more flash-red fluorescence in the Fe-CDC + Magnet group (Fig. 4D) than in the Fe-CDC group (Fig. 4C). Fluorescence intensity was ~4-fold greater in the Fe-CDC + Magnet group (Fig. 4E). At the 3 week time point, fluorescence intensity will reflect the amount of SPMs in the tissue, but not necessarily the number of engrafted CDCs. By this time, transplanted cells may have died, leaving behind their SPMs in the interstitium or in macrophages; alternatively, exocytosis might allow surviving cells to extrude the particles[19]. Given such considerations, the fact that both PCR and FLI give similar values for "engraftment" is remarkable and quite possibly fortuitous. Nevertheless, it is clear that that magnetic targeting increases both short-term (24 hours) and long-term Fe-CDC engraftment (3 weeks) in the injured myocardium.

Magnetically-Targeted Cell Delivery Attenuates Left Ventricular Remodeling and Enhances the Therapeutic Benefit of Cell Transplantation

Morphometric analysis[22] of explanted hearts (n=5-6 from each group) at 3 weeks showed severe LV chamber dilatation and infarct wall thinning in PBS-injected hearts (Fig. 5A). In contrast, the three cell treated groups (Figs. 5B-D) exhibited attenuated LV remodeling. The protective effect was greatest in the Fe-CDC+Magnet group, which had more viable myocardium (Fig. 5E) and thicker infarcted walls (Fig. 5G), but smaller scars (Fig. 5F) and less LV expansion (Fig. 5H). The Fe-CDC and CDC groups were indistinguishable in these measures, indicative of a similar treatment effect in those two groups.

To investigate whether improved cell retention/engraftment translates to enhanced functional benefit, global LVEF was assessed by echocardiography at baseline (Day 0 after MI and cell injection) and 3 weeks later. LVEF at baseline did not differ between treatment groups, indicating a comparable degree of initial injury (Fig. 6A). Over the three weeks after infarction, LVEF declined progressively in the control group (PBS-injected animals) (Fig. 6A), while LVEF improved in all three groups receiving CDCs. These results confirm previous data showing that cardiac function can be significantly improved by transplantation of CDCs[6, 18, 24, 25]. Notably, the Fe-CDC + Magnet group exhibited better cardiac function compared to either the Fe-CDC group or the CDC group (Fig. 6A, $p<0.01$). The LVEFs in the Fe-CDC and CDC groups were indistinguishable, again demonstrating that SPM loading did not undermine the salutary effects of CDCs. To facilitate comparisons among groups, we calculated the treatment effect, i.e. the change in LVEF at 3 weeks relative to baseline, in each group (Fig. 6B). PBS injection had a negative treatment effect, as the LVEF decreased over time, consistent with previous work[6, 18, 24]. In contrast, the Fe-CDC + Magnet group exhibited a sizable positive treatment effect, greater than that in either the Fe-CDC or CDC groups. The treatment effect in the Fe-CDC group was no different than that in the CDC group. In addition, injection of SPMs alone (no cells) had no beneficial effects (Online Fig. IV). To further investigate the relationships between long-term cell retention or myocardial viability on one hand, and cardiac function on the other, 3-week LVEFs were plotted individually against percentages of engraftment (Fig. 6C) or viable myocardium in the risk region (Fig. 6D) at 3 weeks. Better heart function was clearly associated with higher cell retention rate ($R^2=0.8086$) and increased myocardial viability ($R^2=6282$) by linear regression analysis. These composite functional results indicate that the improved cell retention and engraftment in the Fe-CDC + Magnet group indeed translated into superior functional benefit and attenuation of LV remodeling.

Magnetic Targeting Enhances Cell Engraftment and Does Not Worsen Inflammation

To further characterize engraftment, hearts from representative animals in each group were harvested 3 weeks after injection and cryo-sectioned for immunohistochemistry. Confocal imaging enabled the detection of transplanted cells (GFP; green); macrophages (CD68; red); and all cell nuclei (DAPI; blue). Figure 7 shows representative confocal images (A: Fe-CDC + magnet; B: Fe-CDC; C: CDC; D: Control). The cell numbers, quantified as positive cells per high power field (HPF; Fig. 7E) reveal more GFP-positive cells in the Fe-CDC + Magnet group compared to the Fe-CDC or CDC groups. These data agree with the PCR results showing greater long-term cell engraftment with magnetic targeting. Interestingly, GFP-positive multi-cellular clusters were frequently observed in the Fe-CDC + magnet group (Fig. 7A). To quantify the effects of magnetic targeting on the spatial distribution of transplanted cells, GFP-positive cells from 50 randomly selected fields (4×10^4 μm^2) were counted and the number of events was plotted against varying cell numbers (Fig. 7F). Not surprisingly, most of the fields examined were devoid of transplanted cells in all three groups. However, the Fe-CDC + Magnet group had more engraftment area (less “empty” area) compared to the Fe-CDC or CDC group ($p<0.05$). The number of fields with 1-3 engrafted cells was indistinguishable among all the three groups. Interestingly, the Fe-CDC + Magnet group had many more fields with 4-10 or >10 engrafted cells than the Fe-CDC or CDC group ($p<0.001$). Thus, magnetic targeting increases engraftment in focally-condensed patches rather than homogeneously.

One potential concern regarding SPMs and magnetic targeting is the possibility of an inflammatory response, but we found that the tissue density of $CD\text{-}68^{POS}$ macrophages was comparable in all three groups (Fig. 7E). These observations indicate that the presence of SPMs in the host tissue did not cause or worsen inflammation. Notably, at the 3 week time point the majority of GFP-positive cells are SPM-negative; only ~10% of transplanted cells still contained SPMs. A shift of SPMs from the transplanted CDCs to resident macrophages was clearly evident when sections were compared at 24 hours versus 3 weeks (Online Fig. V). These

observations are consistent with the concept that Fe-CDCs expel SPMs via exocytosis *in vivo*, as occurs with other iron-labeled stem cells[26-28], followed by endocytosis by macrophages and eventual incorporation into body's iron stores[29].

We have found that CDCs improve cardiac function both by direct regeneration and by indirect mechanisms[25]. To assess whether transplanted Fe-CDCs differentiate, we stained for cardiac (α-sarcomeric actin) and endothelial (von Willebrand factor) markers. GFP^{POS}/alpha-SA^{POS} cells were consistently detected (Fig. 8A), indicating the ability of transplanted cells to differentiate into cardiomyocytes. The Fe-CDC+Magnet group had more GFP^{POS}/alpha-SA^{POS} and GFP^{NEG}/alpha-SA^{POS} cells than the CDC or Fe-CDC group (Figs. 8B and C). The increase in GFP^{POS}/alpha-SA^{POS} cells attests to the creation of new myocardium by direct differentiation, while the increase in GFP^{NEG}/alpha-SA^{POS} cells likely reflects indirect mechanisms (recruitment of endogenous regeneration and/or tissue preservation)[22, 25, 30]. To further dissect the mechanism of benefit of magnetic targeting, we quantified the magnet-related increment in various cell populations: recipient-derived myocytes, mature donor-derived myocytes and immature donor-derived myocytes (Fig. 8D). Binucleation was used to distinguish between mature and immature myocytes[31]; such myocytes were distinctly longer than mononucleated myocytes, with a typical length:width ratio >3:1. Direct regeneration (GFP^{POS}/alpha-SA^{POS} cells) contributed 17.7% of the total benefit; of that percentage, an absolute 7.3% was comprised of mature donor-derived myocytes. In relative terms, 41.2% of the total donor-derived myocytes were binucleated. The quantitative data also suggest that SPM labeling has minimal impact on *in vivo* cardiac differentiation, as the CDC and Fe-CDC groups had similar densities of GFP^{POS}/alpha-SA^{POS} cells (Fig. 8B). In addition, remnant SPMs in the cytoplasm did not prevent Fe-CDCs from differentiating into a cardiomyocyte phenotype, as SPM/GFP/alpha-SA triple positive cells were detected (Online Fig. VI; highlighted with white solid arrowheads). Endothelial differentiation was also confirmed by the presence of GFP^{POS}/vWF^{POS} cells (Online Fig. VII).

Discussion

One of the main hurdles for cellular cardiomyoplasty is the low, variable retention of transplanted cells[6, 7, 32]. Many injected cells are lost due to the combination of tissue blood flow (washing out cells) and cardiac contraction (squeezing out cells)[6]. Here, we have demonstrated that brief (10 min) magnetic attraction successfully attenuates cell loss during injection. Notably, this transient magnetic targeting seemed to have a “butterfly effect” on subsequent cell therapy outcomes: both functional benefit (Fig. 6) and long-term cell engraftment (Figure 7) were enhanced. We rationalize these findings as follows (see Fig. 8E for a schematic): magnetic targeting improved short-term cell retention (Fig. 4A), which boosted long-term engraftment (Fig. 4B; Fig. 7A). The enhanced engraftment translated into greater therapeutic benefit (Fig. 6) by both indirect (paracrine) and direct regeneration mechanisms, with the former as the dominant factor (Fig. 8D). We also found that some of the CDCs surviving at 3 weeks appear in multi-cellular clusters (Figs. 7A & F) in the Fe-CDC + Magnet group, which we speculate may reflect a condensation effect of magnetic targeting. Three-dimensional multi-cellular clusters are generally more resistant to hostile environments, such as the infarcted myocardium, providing mechanical and paracrine support to transplanted neighbors[33, 34].

This is the first study to report magnetically-targeted cell therapy for enhanced myocardial regeneration. Previous investigations of magnetically-targeted cell delivery for cardiovascular applications are limited to endothelial-related cell therapies such as stent endothelialization or vascular repair[9-15]. In those cases, rheological forces in large-bore vessels are the major obstacle for magnetic targeting to counter. In a myocardial infarction model, venous efflux is potentiated by the squeezing effect of cardiac contraction. We showed that magnetic targeting

can offset the forces driving injected cells out of the myocardium, thereby improving cell engraftment. In addition, previous studies limited their investigation to comparisons of acute cell targeting or retention, without examining possible functional benefits of magnetic targeting. We found that higher cell retention indeed translates into higher engraftment and greater functional improvement downstream. Indeed, the quantitative relationship between engraftment and LV function is striking (Fig. 6C), validating the strategy of boosting cell retention as a means to enhance functional benefit.

The SPMs used in the present studies represent a class of superparamagnetic iron oxides (SPIOs). FDA-approved SPIOs are nontoxic, biocompatible and have been used as MRI contrast agents in human subjects[29, 35]. Consistent with the literature[9, 10], our *in vitro* toxicity data confirmed that micron-size SPIOs had a good safety profile, as they did not significantly alter cell viability, proliferation, adhesion, apoptosis or antigenic phenotype (Fig. 2). Also, SPM labeling did not undermine Fe-CDC proliferation (Figs. 4A and B) or the potential for cardiac and endothelial differentiation (Online Figs. VI and VII) *in vivo*. These findings are consistent with previous characterization of SPIOs in embryonic stem cells[36]. Magnetic targeting did not increase macrophage infiltration (Fig. 7E), consistent with previous work[37, 38]. The potential for chemical toxicity of parenteral iron has also been well documented[39]. Iron from injected SPMs will eventually be incorporated into the body's own iron stores. The total amount of iron oxide for diagnostic imaging (40-200 mg Fe) is small compared to the total human iron stores (around 3500 mg). The amount needed for magnetically-targeted cell therapy will likely be even smaller. For instance, in the ongoing phase I clinical trial CADUCEUS (see www.clinicaltrials.org), we give a maximum of 25 million CDCs to each study subject. Based on the fact that every SPM particle contains 0.5 pg of iron oxides and a 500:1 SPM to cell ratio is used, only 5 mg of Fe would be administered to each patient treated with such a protocol.

We employed direct myocardial injection in this study because it is a well-characterized cell delivery method in small animal models. However, less-invasive routes such as intravenous or intracoronary delivery also stand to benefit from magnetic targeting. Such routes of delivery yield even lower cell retention rates than direct myocardial injection[40, 41]. In pondering the translation of our results to a clinical setting, we envision non-invasive exposure to magnetic fields near the heart while cell delivery is performed. The external magnetic field may be generated as simply as by applying a fixed magnet to the patient's chest, although machines that focus and potentially shape the magnetic field may enable more refinement, extending to specific regions within the body (e.g., the posterior wall of the heart)[42]. Electromagnetic catheters represent another potential means of focused field generation within defined regions of the body.

We conclude that magnetic targeting enhances cell retention, engraftment and functional benefit in a rat myocardial infarction model. While describing a new and promising method, the present study has a number of limitations: we have employed only a proof-of-concept small animal model; further optimization is needed to find the best magnetic strength and duration for effective targeting; and large-animal data are necessary in order to advance the process of translation. In addition, rather than optimizing basal cell dosage, we chose a number consistent with various prior studies[6, 22, 43] that had shown functional benefit in small animals. We recognize that the dosages used here may not be readily scalable to the clinical setting. Further dosage optimization would be valuable, both in small- and large-animal models, in order to inform future clinical studies.

Novelty and Significance

“What is known?”

- When cells are injected into the heart, the retention of injected cells in the tissue is low, potentially restricting the therapeutic benefit of cardiomyoplasty.
- Cardiosphere-derived cells (CDCs) improve cardiac function in the injured heart and exhibit multilineage potential.
- While CDCs can engraft and differentiate into cardiomyocytes and vascular cells in the injured heart, most of their therapeutic benefit is attributable to indirect ("paracrine") mechanisms rather than to direct regeneration.

"What new information does this article contribute?"

- Loading cardiosphere-derived cells with iron oxide particles renders them susceptible to magnetic attraction but does not interfere with their viability or function.
- Brief external magnetic field application as an adjunct to magnetized CDC injection ("magnetic targeting") triples short-term retention as well as long-term engraftment.
- Adverse remodeling of the heart is attenuated, viability is enhanced, and ventricular function is greater with magnetic targeting.
- Greater cell retention leads to superior benefits via scaling of previously-described mechanisms (paracrine effects plus a minor contribution of direct regeneration).

Summary

The success of stem cell therapies for heart disease is limited by low transplanted cell retention in the tissue, due at least in part to washout via coronary veins. We sought to counter the efflux of transplanted cells by rendering them magnetically-responsive and imposing an external magnetic field on the heart during and immediately after injection. CDCs were labeled with superparamagnetic microspheres, a process which did not undermine cell viability or function. Labeled rat CDCs were injected into the peri-infarct region in rats undergoing acute myocardial infarction. When a magnet was superimposed on the surgical field to achieve magnetic targeting, cells were visibly attracted towards the magnet and accumulated around the ischemic zone. In contrast, the majority of non-targeted cells washed out immediately after injection. More transplanted cells were retained in the heart, and fewer migrated into other organs, with magnetic targeting; adverse ventricular remodeling was attenuated, and functional improvement was superior. This simple, novel method to improve injected cell retention is readily generalizable, and offers the potential for rapid translation to clinical applications.

Supplementary Material

Refer to Web version on PubMed Central for supplementary material.

Acknowledgments

The authors thank Christy Houde, Supurna Chowdhury and Giselle Galang for technical assistance. We also thank Drs. John Terrovitis and Rachel Smith for helpful discussions.

Source of Funding: Supported by NIH R01 HL083109.

Non-Standard Abbreviations and Acronyms

alpha-SA	alpha-sarcomeric actin
CDC	cardiosphere-derived cell
GFP	green fluorescent protein
IC	intracoronary
IV	intravenous
LV	left ventricle
LVEF	left ventricular ejection fraction
MI	myocardial infarction
ROS	reactive oxygen species
SPM	superparamagnetic microsphere
SPIO	superparamagnetic iron oxides
WKY	Wistar Kyoto
vWF	Von Willebrand factor

References

1. Wollert KC, Drexler H. Clinical Applications of Stem Cells for the Heart. Circ Res 2005;96:151–163. [PubMed: 15692093]
2. Fukushima S, Varela-Carver A, Coppen SR, Yamahara K, Felkin LE, Lee J, Barton PJR, Terracciano CMN, Yacoub MH, Suzuki K. Direct Intramyocardial But Not Intracoronary Injection of Bone Marrow Cells Induces Ventricular Arrhythmias in a Rat Chronic Ischemic Heart Failure Model. Circulation 2007;115:2254–2261. [PubMed: 17438152]
3. Robey TE, Saiget MK, Reinecke H, Murry CE. Systems approaches to preventing transplanted cell death in cardiac repair. Journal of Molecular and Cellular Cardiology 2008;45:567–581. [PubMed: 18466917]
4. Ye L, Haider HK, Guo C, Sim EKW. Cell-Based VEGF Delivery Prevents Donor Cell Apoptosis After Transplantation. The Annals of Thoracic Surgery 2007;83:1233–1234. [PubMed: 17307513]
5. Zhang M, Methot D, Poppa V, Fujio Y, Walsh K, Murry CE. Cardiomyocyte Grafting for Cardiac Repair: Graft Cell Death and Anti-Death Strategies. Journal of Molecular and Cellular Cardiology 2001;33:907–921. [PubMed: 11343414]
6. Terrovitis J, Bonios M, Fox J, Engles JM, Yu J, Leppo MK, Pomper MG, Wahl RL, Seidel J, Tsui BM, Bengel FM, Abraham R, Marban E. Noninvasive Quantification and Optimization of Acute Cell Retention by In Vivo Positron Emission Tomography After Intramyocardial Cardiac-Derived Stem Cell Delivery. Journal of the American College of Cardiology 2009;54:1619–1626. [PubMed: 19833262]
7. Teng CJ, Luo J, Chiu RCJ, Shum-Tim D. Massive mechanical loss of microspheres with direct intramyocardial injection in the beating heart: Implications for cellular cardiomyoplasty. The Journal of Thoracic and Cardiovascular Surgery 2006;132:628–632. [PubMed: 16935119]
8. Polyak B, Friedman G. Magnetic targeting for site-specific drug delivery: applications and clinical potential. Expert Opinion on Drug Delivery 2009;6:53–70. [PubMed: 19236208]
9. Pislaru SV, Harbuzariu A, Agarwal G, Witt Aas Cvt Latg T, Gulati R, Sandhu NP, Mueske Aa C, Kalra M, Simari RD, Sandhu GS. Magnetic Forces Enable Rapid Endothelialization of Synthetic Vascular Grafts. Circulation 2006;114:I-314–318. [PubMed: 16820592]
10. Pislaru SV, Harbuzariu A, Gulati R, Witt T, Sandhu NP, Simari RD, Sandhu GS. Magnetically Targeted Endothelial Cell Localization in Stented Vessels. Journal of the American College of Cardiology 2006;48:1839–1845. [PubMed: 17084259]

11. Polyak B, Fishbein I, Chorny M, Alferiev I, Williams D, Yellen B, Friedman G, Levy RJ. High field gradient targeting of magnetic nanoparticle-loaded endothelial cells to the surfaces of steel stents. Proceedings of the National Academy of Sciences 2008;105:698–703.
12. Singh JP. Enabling Technologies for Homing and Engraftment of Cells for Therapeutic Applications. J Am Coll Cardiol Intv 2009;2:803–804.
13. Sorin VP, Adriana H, Rajiv G, Tyra W, Nicole PS, Robert DS, Gurpreet SS. Magnetically Targeted Endothelial Cell Localization in Stented Vessels. Journal of the American College of Cardiology 2006;48:1839–1845. [PubMed: 17084259]
14. Kyrtatos PG, Lehtolainen P, Junemann-Ramirez M, Garcia-Prieto A, Price AN, Martin JF, Gadian DG, Pankhurst QA, Lythgoe MF. Magnetic Tagging Increases Delivery of Circulating Progenitors in Vascular Injury. J Am Coll Cardiol Intv 2009;2:794–802.
15. Consigny P, Silverberg D, Vitali N. Use of endothelial cells containing superparamagnetic microspheres to improve endothelial cell delivery to arterial surfaces after angioplasty. J Vasc Interv Radiol 1999;10:155–163. [PubMed: 10082102]
16. Davis DR, Zhang Y, Smith RR, Cheng K, Terrovitis J, Malliaras K, Li TS, White A, Makkar R, Marban E. Validation of the Cardiosphere Method to Culture Cardiac Progenitor Cells from Myocardial Tissue. PLoS ONE 2009;4:e7195. [PubMed: 19779618]
17. Messina E, De Angelis L, Frati G, Morrone S, Chimenti S, Fiordaliso F, Salio M, Battaglia M, Latronico MVG, Coletta M, Vivarelli E, Frati L, Cossu G, Giacomello A. Isolation and Expansion of Adult Cardiac Stem Cells From Human and Murine Heart. Circ Res 2004;95:911–921. [PubMed: 15472116]
18. Smith RR, Barile L, Cho HC, Leppo MK, Hare JM, Messina E, Giacomello A, Abraham MR, Marban E. Regenerative Potential of Cardiosphere-Derived Cells Expanded From Percutaneous Endomyocardial Biopsy Specimens. Circulation 2007;115:896–908. [PubMed: 17283259]
19. Terrovitis J, Stuber M, Youssef A, Preece S, Leppo M, Kizana E, Schar M, Gerstenblith G, Weiss RG, Marban E, Abraham MR. Magnetic Resonance Imaging Overestimates Ferumoxide-Labeled Stem Cell Survival After Transplantation in the Heart. Circulation 2008;117:1619–1626.
20. Kanoh M, Takemura G, Misao J, Hayakawa Y, Aoyama T, Nishigaki K, Noda T, Fujiwara T, Fukuda K, Minatoguchi S, Fujiwara H. Significance of Myocytes With Positive DNA In Situ Nick End-Labeling (TUNEL) in Hearts With Dilated Cardiomyopathy : Not Apoptosis but DNA Repair. Circulation 1999;99:2757–2764. [PubMed: 10351969]
21. Cheng Z, Levi J, Xiong Z, Gheysens O, Keren S, Chen X, Gambhir SS. Near-Infrared Fluorescent Deoxyglucose Analogue for Tumor Optical Imaging in Cell Culture and Living Mice. Bioconjugate Chemistry 2006;17:662–669. [PubMed: 16704203]
22. Tang XL, Rokosh G, Sanganalmath SK, Yuan F, Sato H, Mu J, Dai S, Li C, Chen N, Peng Y, Dawn B, Hunt G, Leri A, Kajstura J, Tiwari S, Shirk G, Anversa P, Bolli R. Intracoronary Administration of Cardiac Progenitor Cells Alleviates Left Ventricular Dysfunction in Rats With a 30-Day-Old Infarction. Circulation 2010;121:293–305. [PubMed: 20048209]
23. Li Z, Lee A, Huang M, Chun H, Chung J, Chu P, Hoyt G, Yang P, Rosenberg J, Robbins RC, Wu JC. Imaging Survival and Function of Transplanted Cardiac Resident Stem Cells. Journal of the American College of Cardiology 2009;53:1229–1240. [PubMed: 19341866]
24. Johnston PV, Sasano T, Mills K, Evers R, Lee ST, Smith RR, Lardo AC, Lai S, Steenbergen C, Gerstenblith G, Lange R, Marban E. Engraftment, Differentiation, and Functional Benefits of Autologous Cardiosphere-Derived Cells in Porcine Ischemic Cardiomyopathy. Circulation 2009;120:1075–1083. [PubMed: 19738142]
25. Chimenti I, Smith RR, Li TS, Gerstenblith G, Messina E, Giacomello A, Marban E. Relative Roles of Direct Regeneration Versus Paracrine Effects of Human Cardiosphere-Derived Cells Transplanted Into Infarcted Mice. Circ Res CIRCRESAHA :109.210682.
26. Arbab AS, Jordan EK, Wilson LB, Yocum GT, Lewis BK, Frank JA. In Vivo Trafficking and Targeted Delivery of Magnetically Labeled Stem Cells. Human Gene Therapy 2004;15:351–360. [PubMed: 15053860]
27. Arbab AS, Bashaw LA, Miller BR, Jordan EK, Lewis BK, Kalish H, Frank JA. Characterization of Biophysical and Metabolic Properties of Cells Labeled with Superparamagnetic Iron Oxide

Nanoparticles and Transfection Agent for Cellular MR Imaging1. Radiology 2003;229:838–846. [PubMed: 14657318]

28. Wang YXJ, Wang HH, Au DWT, Zou BS, Teng LS. Pitfalls in employing superparamagnetic iron oxide particles for stem cell labelling and in vivo MRI tracking. Br J Radiol 2008;81:987-a–988. [PubMed: 19029055]
29. Thorek D, Chen A, Czupryna J, Tsourkas A. Superparamagnetic Iron Oxide Nanoparticle Probes for Molecular Imaging. Annals of Biomedical Engineering 2006;34:23–38. [PubMed: 16496086]
30. Gnecchi M, Zhang Z, Ni A, Dzau VJ. Paracrine Mechanisms in Adult Stem Cell Signaling and Therapy. Circ Res 2008;103:1204–1219. [PubMed: 19028920]
31. Chen X, Wilson RM, Kubo H, Berretta RM, Harris DM, Zhang X, Jaleel N, MacDonnell SM, Bearzi C, Tillmanns J, Trofimova I, Hosoda T, Mosna F, Cribbs L, Leri A, Kajstura J, Anversa P, Houser SR. Adolescent Feline Heart Contains a Population of Small, Proliferative Ventricular Myocytes With Immature Physiological Properties. Circ Res 2007;100:536–544. [PubMed: 17272809]
32. Adil Al Kindi YG, Shum-Tim Dominique, Ray CJ. Chiu cellular cardiomyoplasty: routes of cell delivery and retention. Frontiers in Bioscience 2008;13:2421–2434. [PubMed: 17981723]
33. Ruei-Zhen Lin HYC. Recent advances in three-dimensional multicellular spheroid culture for biomedical research. Biotechnology Journal 2008;3:1172–1184. [PubMed: 18566957]
34. Chung-Chi W, Chun-Hung C, Shiaw-Min H, Wei-Wen L, Chih-Hao H, Wen-Yu L, Yen C, Hsing-Wen S. Spherically Symmetric Mesenchymal Stromal Cell Bodies Inherent with Endogenous Extracellular Matrices for Cellular Cardiomyoplasty. Stem Cells 2009;27:724–732. [PubMed: 19259939]
35. Corot C, Robert P, Idée JM, Port M. Recent advances in iron oxide nanocrystal technology for medical imaging. Advanced Drug Delivery Reviews 2006;58:1471–1504. [PubMed: 17116343]
36. Au KW, Liao SY, Lee YK, Lai WH, Ng KM, Chan YC, Yip MC, Ho CY, Wu EX, Li RA, Siu CW, Tse HF. Effects of iron oxide nanoparticles on cardiac differentiation of embryonic stem cells. Biochemical and Biophysical Research Communications 2009;379:898–903. [PubMed: 19135029]
37. Bourrinet PP, Bengele HHP, Bonnemain BP, Dencausse AP, Idee JMP, Jacobs PMBSP, Lewis JMP. Preclinical Safety and Pharmacokinetic Profile of Ferumoxtran-10, an Ultrasmall Superparamagnetic Iron Oxide Magnetic Resonance Contrast Agent. Investigative Radiology 2006;41:313–324. [PubMed: 16481915]
38. Raynal IP, Prigent PP, Peyramaure SBS, Najid AP, Rebuzzi CMS, Corot CP. Macrophage Endocytosis of Superparamagnetic Iron Oxide Nanoparticles: Mechanisms and Comparison of Ferumoxides and Ferumoxtran-10. Investigative Radiology 2004;39:56–63. [PubMed: 14701989]
39. Bonnemain B. Superparamagnetic Agents in Magnetic Resonance Imaging: Physicochemical Characteristics and Clinical Applications A Review. Journal of Drug Targeting 1998;6:167–174. [PubMed: 9888302]
40. Freyman T, Polin G, Osman H, Crary J, Lu M, Cheng L, Palasis M, Wilensky RL. A quantitative, randomized study evaluating three methods of mesenchymal stem cell delivery following myocardial infarction. Eur Heart J 2006:ehi818.
41. Hou D, Youssef EAS, Brinton TJ, Zhang P, Rogers P, Price ET, Yeung AC, Johnstone BH, Yock PG, March KL. Radiolabeled Cell Distribution After Intramyocardial, Intracoronary, and Interstitial Retrograde Coronary Venous Delivery: Implications for Current Clinical Trials. Circulation 2005;112:I-150–156. [PubMed: 16159808]
42. Ernst S, Ouyang F, Linder C, Hertting K, Stahl F, Chun J, Hachiya H, Bansch D, Antz M, Kuck KH. Initial Experience With Remote Catheter Ablation Using a Novel Magnetic Navigation System: Magnetic Remote Catheter Ablation. Circulation 2004;109:1472–1475. [PubMed: 15023876]
43. Haider HK, Jiang S, Idris NM, Ashraf M. IGF-1-Overexpressing Mesenchymal Stem Cells Accelerate Bone Marrow Stem Cell Mobilization via Paracrine Activation of SDF-1{alpha}/CXCR4 Signaling to Promote Myocardial Repair. Circ Res 2008;103:1300–1308. [PubMed: 18948617]

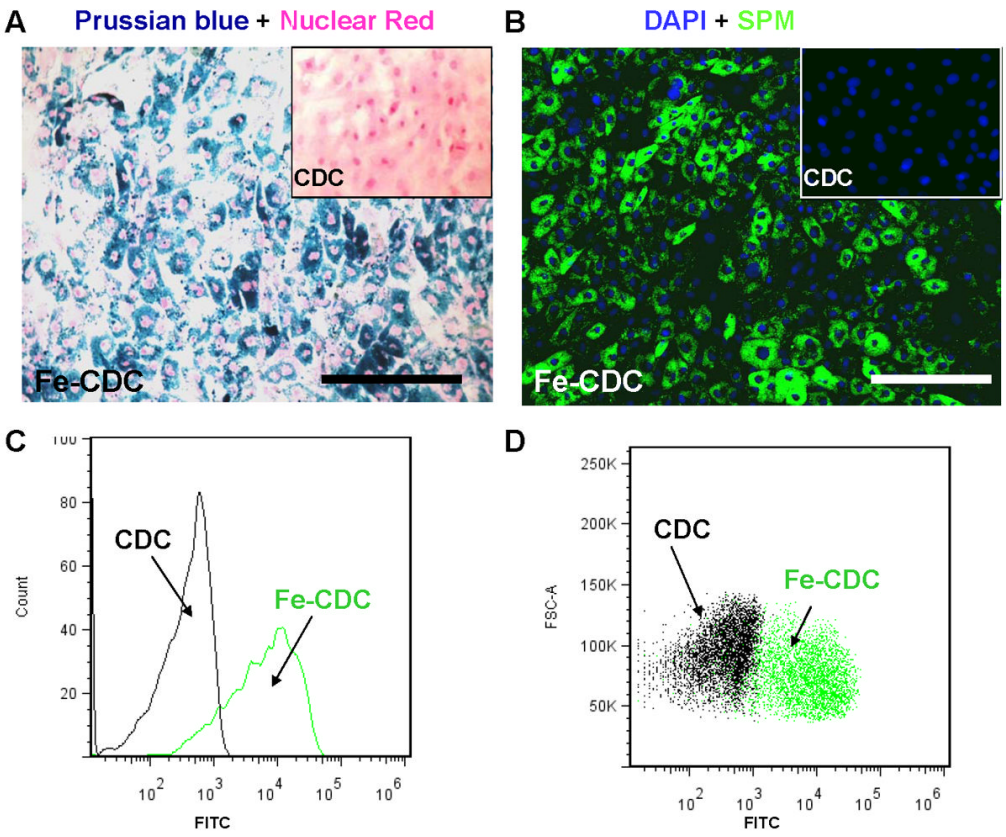

Figure 1.

SPM labeling of CDCs. A, rat CDCs were co-incubated with SPMs for 24 hours at a 500:1 SPM: cell ratio. The cells were then fixed, stained for Prussian Blue (iron) and counter-stained with nuclear red. B, CDCs were labeled with dragon-green-conjugated SPMs for 24 hours and then examined by fluorescence microscopy. Non-labeled cells did not express Prussian Blue or Dragon-green fluorescence (Insets, A&B). C and D, representative flow cytometry histogram and dot plots of SPM-labeled (green) and non-labeled CDCs (black). Bars = 100 μm in A and B.

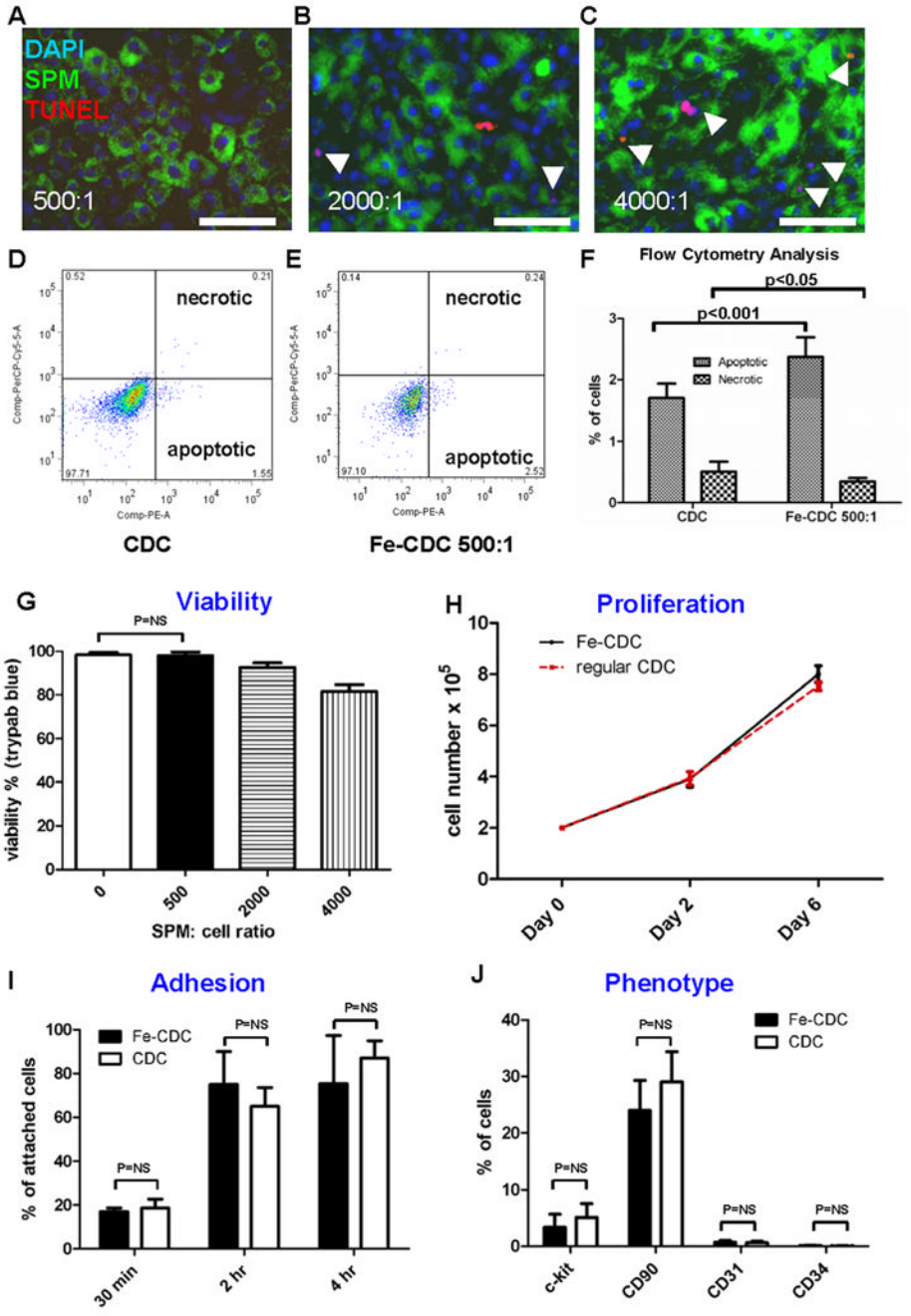

Figure 2.

Effects of SPM labeling on cell death and function. A-C, microscopy images of TUNEL staining (Red: apoptotic cells; green: SPMs; blue: nuclei). CDCs were co-incubated with SPMs for 24 hours at varying SPM:cell ratios: 500:1 (A); 2000:1 (B); 4000:1 (C). Apoptotic cells (red color) are highlighted with white arrowheads. Bars = 50 μm. D and E, Typical plots of Annexin/7-AAD flow cytometry from non-labeled CDCs (D) and SPM-labeled CDCs (E). F, quantification of apoptotic and necrotic cells by flow cytometry (n=9 for CDC; n=8 for Fe-CDC). CDCs were labeled with SPMs for 24 hours and then examined for viability and function. G, viability of SPM-labeled CDCs assessed by Trypan Blue exclusion. Viability decrease was only observed in the 2000:1 and 4000:1 dosage groups, but not in the 500:1 group.

H, proliferation of Fe-CDCs (labeled at 500:1 SPMs) compared with that of control CDCs (n=4). Cell counts at Day 0, 2 and 6 were equivalent in the two groups. I, adhesion potency of Fe-CDCs (labeled with 500:1 SPMs) compared with that of control CDCs (n=3). Attached cell numbers at 30 min, 2 hours and 4 hours were not statistically different in the two groups. J, phenotypic markers c-kit, CD90, CD31 and CD34 from Fe-CDCs (n=8) were compared to those from control CDCs (n=9). No statistical differences were detected for any of those markers.

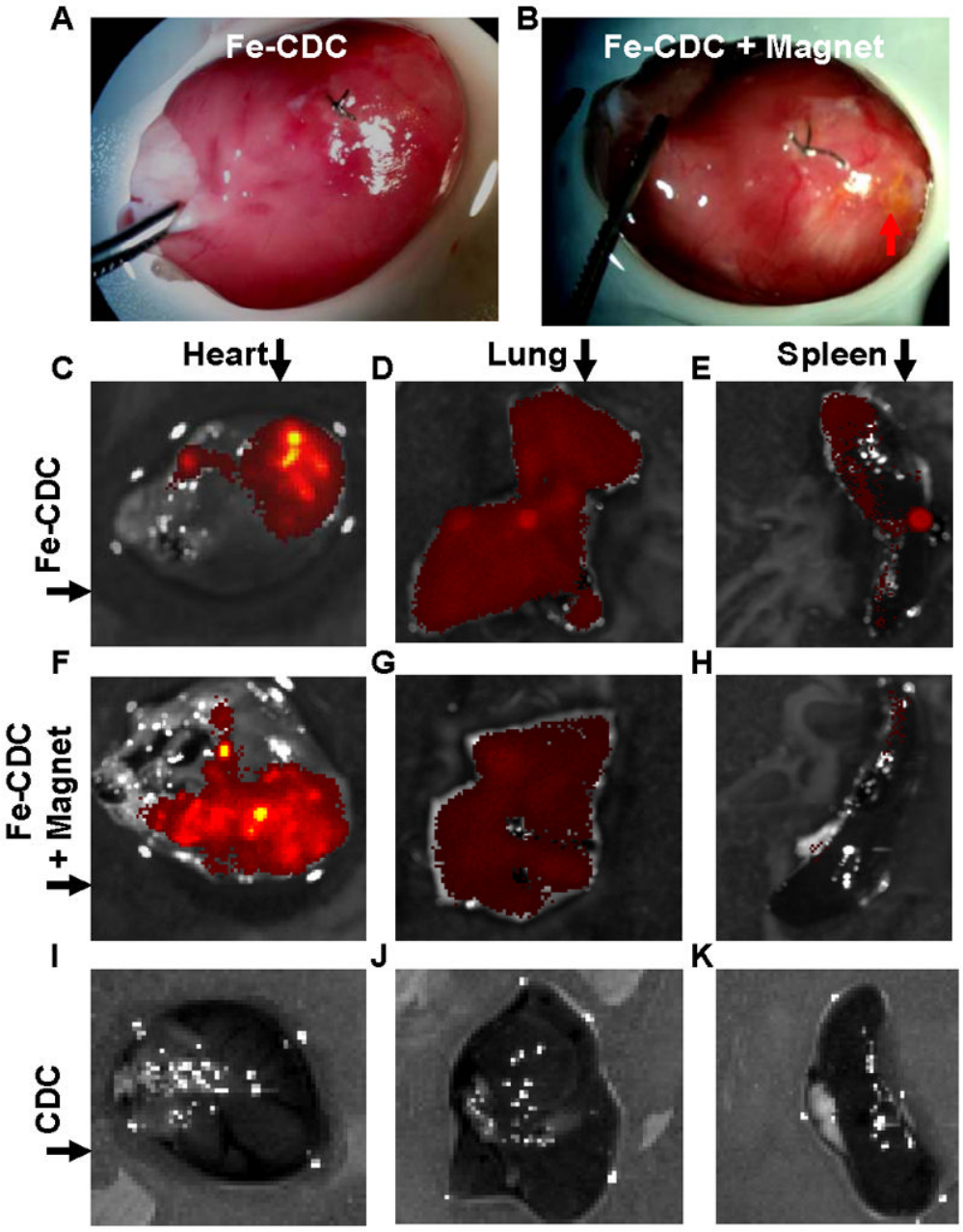

Figure 3.

Magnetic targeting increases short-term cell retention in the hearts and reduces off-target migration. A and B: Representative images of hearts from the Fe-CDC and Fe-CDC + Magnet group 24 hours after cell injection. Cells are visible as a yellow-brown area in the Fe-CDC + Magnet group (B; red arrow) but not in the Fe-CDC group (A). C-K: Representative fluorescence imaging of organs harvested at 24 hours after cell injection. CDCs were labeled with flash-red-conjugated SPMs. Exposure time was set at the same level for each imaging procedure. More fluorescence was detected in a heart from the Fe-CDC + Magnet group (F) than in the Fe-CDC group (C). Red fluorescence signals were detectable in the lungs and spleens, but less so in the lungs and spleens from the Fe-CDC + Magnet group (G and H) than in those from the Fe-CDC group (D and E). As a negative control, excised organs from the

CDC group (animals were injected with non-labeled cells) were also imaged; no signals were detected from any such organs (I-K).

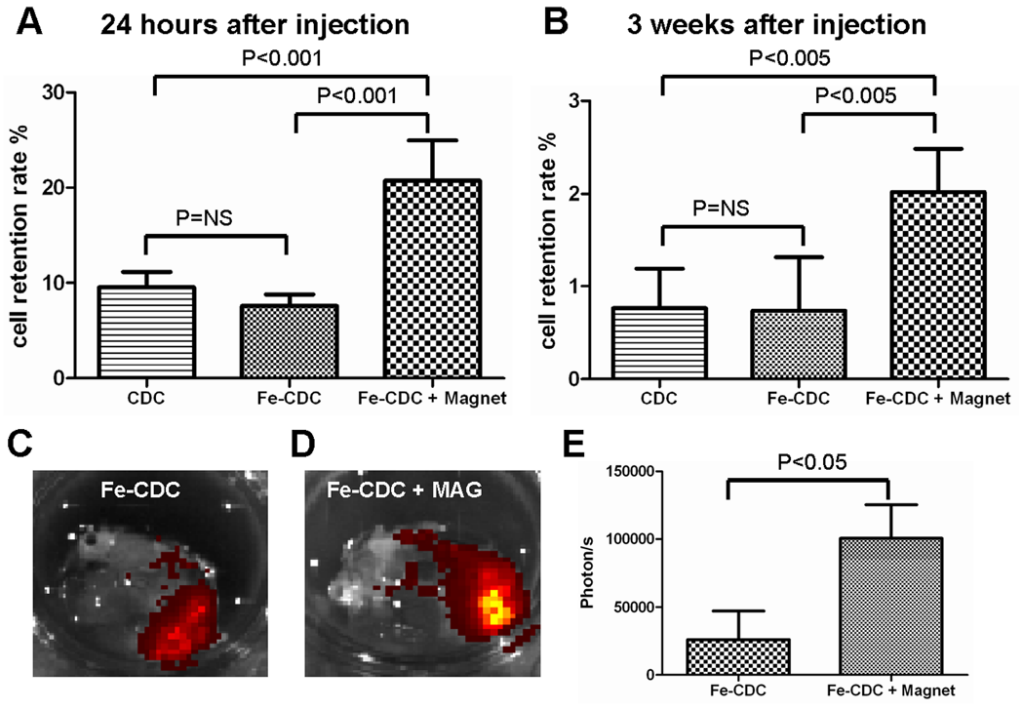

Figure 4.

Effects of magnetic targeting on short-term cell retention and long-term cell engraftment. A, female animals (n=6) were sacrificed 24 hours after cell injection. Donor male cells persistent in the female hearts were detected by quantitative PCR for the SRY gene. B, similar PCR experiment performed 3 weeks after injection. C and D, CDCs were labeled with flash-red-conjugated SPMs and then injected into animals with (D) or without (C) magnetic targeting. At 3 weeks after injection, representative hearts from both groups (n=3) were harvested and imaged for detection of flash-red fluorescence. More fluorescence is evident in the Fe-CDC +Magnet heart. E, fluorescence intensities (photon/s) from a fixed region of interest (ROI) measured with the Xenogen software.

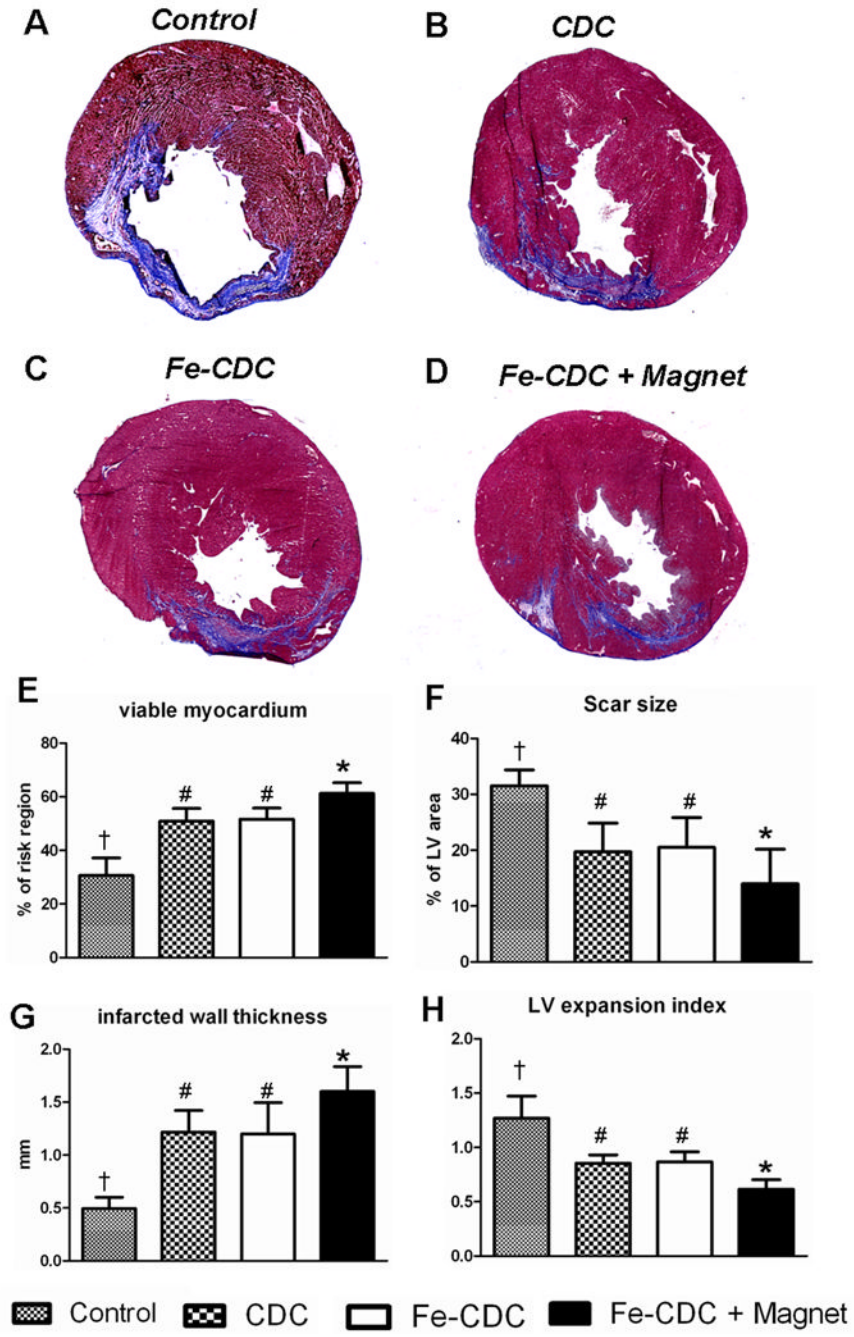

Figure 5.

Morphometric heart analysis. A-D, Representative Masson's trichrome-stained myocardial sections from a subgroup of animals at 3 weeks after treatment (n=6 for Fe-CDC+Magnet and Fe-CDC; n=5 for CDC and Control). Scar tissue and viable myocardium are identified in blue and red color, respectively. E-H, quantitative analysis and LV morphometric parameters (for definition and calculation methods, please see Supplemental Materials-Detailed Methods). † indicates P<0.05 when compared to any other groups. # indicates P=NS. * indicates P<0.05 when compared to any other groups.

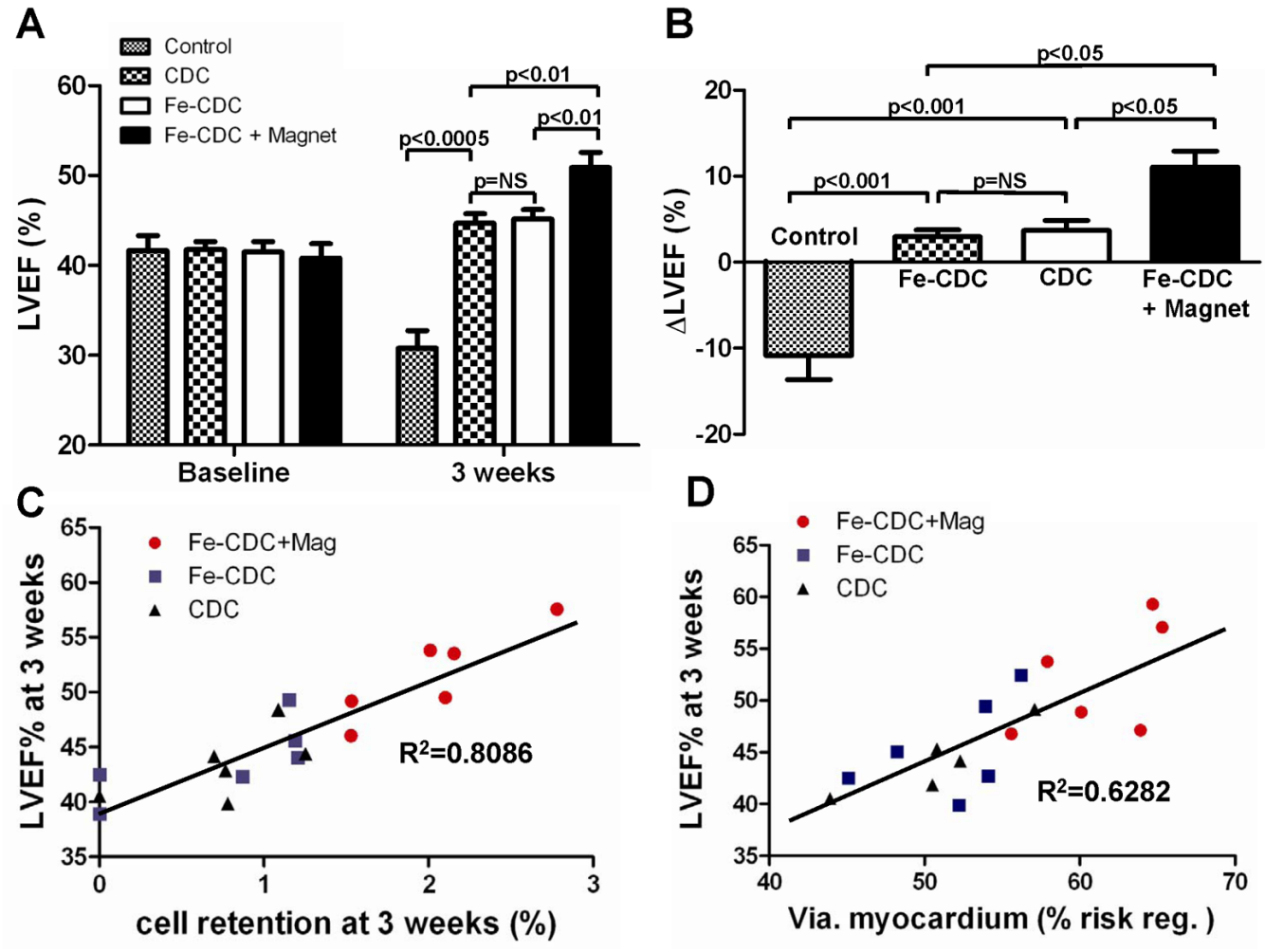

Figure 6.

Magnetic targeting enhances functional benefit of CDC transplantation. A, left ventricular ejection fraction (LVEF) measured by echocardiography at baseline and 3 weeks after cell injection (n=12 for Fe-CDC+Magnet and Fe-CDC; n=11 for CDC; n=9 for Control). Baseline LVEFs were indistinguishable among the four groups. 2-tailed paired student *t*-test revealed that all three cell-treated groups had LVEF improvement, while the LVEF from the control group decreased from baseline. The functional improvement was greater in the Fe-CDC +Magnet group than in the others. B, Changes of LVEF from baseline in each group. Values are expressed as mean ± S.E.M. C & D, 3-week LVEFs were plotted against 3-week cell retention rates and viable myocardium in the risk region, from each animal in each group for which both sets of data were available. Linear regression was performed.

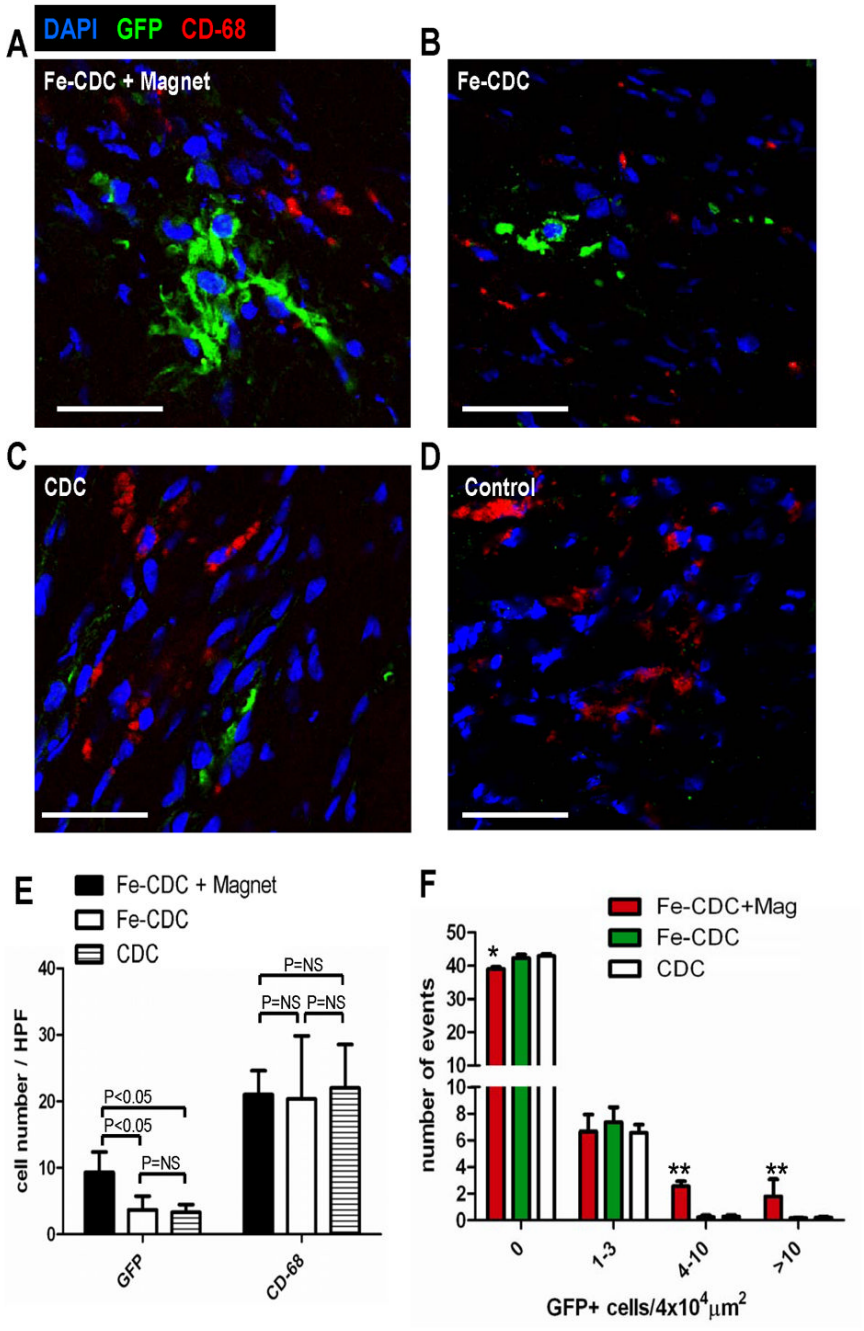

Figure 7.

Histological analysis of cell engraftment and inflammatory response. At 3 weeks after cell transplantation, hearts from representative animals (n=5-6) in each group were harvested and frozen-sectioned for histological analysis. Sections from different depths of the heart were stained for CD-68 (macrophages) and counter-stained with DAPI. Confocal imaging was performed for simultaneous detection of transplanted cells (GFP; green) and macrophages (CD-68; red): A, Fe-CDC+magnet; B, Fe-CDC; C, CDC; D, Control. Bars=100 μm. E, GFP-positive cell and macrophage numbers from 6 randomly-selected high power fields (3 from infarct area and 3 from peri-infarct area) on each section were quantified. F, GFP-positive cells in 50 randomly selected fields ($4\times10^4\mu m^2$) were counted. The number of events was plotted

against varying GFP-positive cell numbers. ** and * indicates $P<0.01$ and $P<0.05$ respectively, when compared to the CDC or Fe-CDC group.

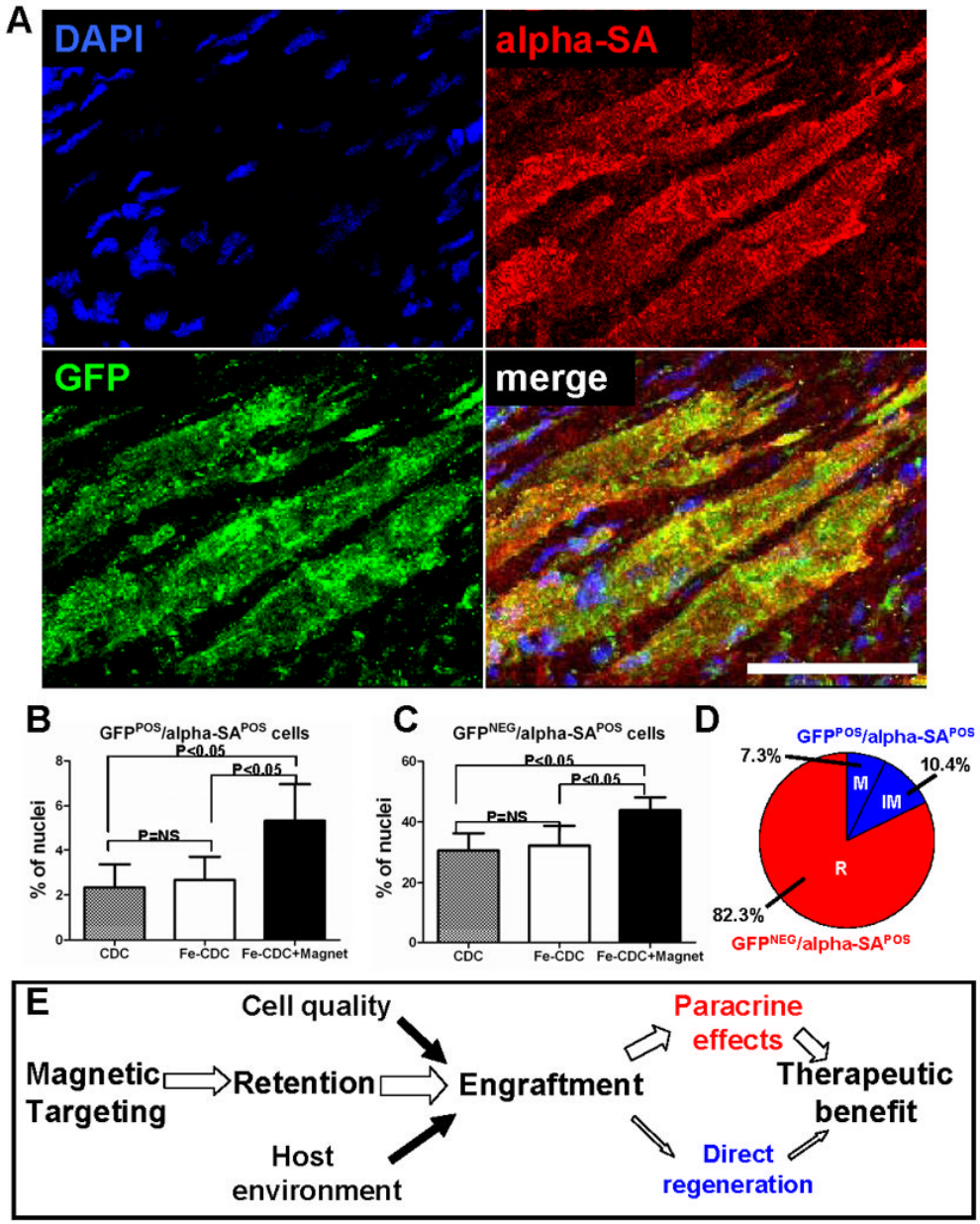

Figure 8. Cardiac differentiation of transplanted CDCs

A, representative confocal micrographs from a heart in the Fe-CDC + Magnet group showing cells expressing GFP (green) and alpha-SA (red). The colocalization of GFP with alpha-SA indicates that transplanted CDCs participated in regeneration of myocardium, differentiating into a cardiomyocyte phenotype. B and C, quantification of the density of GFP^{POS}/alpha-SA^{POS} and GFP^{NEG}/alpha-SA^{POS} cells in the regions where GFP cells engrafted. D, The percentage distribution of recipient and donor myocytes (both mature and immature) in the increment from the Fe-CDC group to the Fe-CDC+Magnet group is quantified. “M”=mature donor-derived cardiomyocytes; “IM”=immature donor-derived cardiomyocytes; “R”=recipient-derived cardiomyocytes. E, potential mechanism of magnetic targeting-enhanced cell therapy. Bar = 50 μm.